The 2013 World Congress on
Advances in Structural Engineering and Mechanics (ASEM13)
Jeju, Korea, September 8-12, 2013

Compressive behavior of hybrid FRP confined concrete columns

*Li-Juan Li[1)], Shun-De Xu[2)], Lan Zeng[3)], Yong-Chang Guo[4)]

[1), 2), 3), 4)] *School of Civil and Transportation Engineering, Guangdong University of Technology, Guangzhou, 510006, China*
[1)] *lilj@gdut.edu.cn*

ABSTRACT

In this paper, the mechanical property of CFRP, BFRP, GFRP and their hybrid FRP were experimentally studied. The elastic module and compressive strength of CFRP, BFRP, GFRP and their hybrid FRP were tested. The experiment results showed that the elastic module of hybrid FRP agreed well with theoretical mixing rule while the tensile strength did not. The bearing capacity, peak strain, stress-strain relationship of circular concrete columns confined by CFRP, BFRP, GFRP and hybrid FRP under axial compressive load were recorded. And the confining effectiveness of hybrid FRP on concrete columns was analyzed. The test results showed that the bearing capacity and ductility of concrete columns were efficiently improved through hybrid FRP confining. A strength model and a stress-strain relationship model of hybrid FRP confined concrete columns were proposed. The proposed stress-strain model was shown to be capable of providing accurate prediction of the behavior of hybrid FRP confined concrete compared with other hybrid FRP model. The new stress-strain simulation model was also suitable for single FRP confinement cases and was easy for use in design of structures.

1. INTRODUCTION

The superior material properties of the fiber reinforced polymer (FRP) composite material, such as light weight, high strength, good corrosion resistance, make it very suitable for strengthening a broad range of structural members, including beams, columns, slabs, masonry and walls. As a result, the past decade has witnessed the fast development of research on the use of FRP materials in civil engineering (Teng et al. 2002, Saadatmanesh and Ehsani 1991, Sundarraja and Prabhu 2012, Chen et al. 2012, Guo et al. 2012, Teng et al. 2012). The advantages and disadvantages of using one kind of FRP materials, such as carbon fiber reinforced polymer (CFRP) , glass fiber

---

[1)] Professor
[2)] Graduate Student
[3)] Graduate Student
[4)] Associate Professor
Note: Copied from the manuscript submitted to "Computers and Concrete, An International Journal" for presentation at ASEM13 Congress

reinforced polymer (GFRP), or basaltic fiber reinforced polymer (BFRP) to strengthen concrete columns are obvious (Meier et al. 1993, Guo et al. 2009, Mosallam et al. 2012, Rousakis and Karabinis 2012). For instance, CFRP can improve the bearing capacity of members effectively with its high elasticity modulus and tensile strength, but it also has the disadvantages of low elongation which results in the low deformation performance of reinforced structures; and the price of CFRP is relatively high. On the contrary, GFRP is low in strength and elasticity modulus, but it has much higher elongation and lower prices, which increases the ductility of the strengthened structures while decreases their cost. Recently, a number of studies about FRP strengthening method are focused on hybrid strengthening program, in which different FRP materials are used to achieve expected strengthening results (Chen et al. 2008, Li et al. 2009, Vanaja and Rao 2002), or to obtain FRP confined new members (Guo et al. 2009).

The studies on using hybrid fiber reinforced polymer (HFRP) to strength concrete members have been mainly focused on HFRP strengthened concrete beams and columns (Li et al. 2009, Lau and Pam 2010). Hosny et al. (2006) found that a single type of FRP can enhance the load-bearing capacity of T-beam strengthened but lower its ductility, while a hybrid use of CFRP and GFRP can improve both the load-bearing capacity and ductility of the strengthened beams. Moreover, Li et al. (2002) studied the behavior of beam-column joins strengthened with FRP and found that HFRP can improve both the stiffness and load-bearing capacity of components, absorb deformation energy and postpone the appearance of concrete cracks. The studies of Bouchelaghem et al. (2011) and Zhao et al. (2013) pointed out that hybrid use of FRPs can effectively increase the load-capacities of the strengthened members, meanwhile increase the ductility of members and thus achieve an optimum use of the materials.

A thorough review of related existing literature reveals that the studies on compressive behavior of HFRP confined concrete structures (especially columns) is limited. Due to the improved ductility of strengthened members which can be obtained with HFRP, the HFRP confined concrete has a special potential to be used in the structures with seismic resistance requirements. The stress-strain relationship of HFRP confined concrete columns is necessary in the aseismic design of structures. Different stress-strain models of FRP confined concrete materials were proposed (Farids and Khalili 1982, Miyauchi et al. 1999 and Samaan et al. 1998), among which the model proposed by Teng et al. (2002) had been accepted by many researcher as an accurate model. Nevertheless, whether the existing models of FRP confined concrete can be extended to predict the behavior of HFRP confined concrete is yet to be confirmed.

Against above background, this paper presents an experiential study on concrete columns confined by three kinds of hybrid FRPs, including CFRP, BFRP and GFRP, with the main aim of study being exploring the confining effect of the hybrid use of FRPs on concrete. The compressive strengths and stress-strain curves of concrete columns confined by HFRP were presented, based on which the performance of FRPs was demonstrated, and a stress-strain model of the concrete confined by HFRP was proposed as well.

2. TEST SPECIMENS

2.1 Design of specimens

In this study, 30 cylinder specimens with a diameter of 150 mm and a height of 300mm were cast for testing as shown in Fig. 1. The average cube compressive strength of concrete was 38.73 MPa. The molds of specimens were removed in 24 hours after pouring, and the specimens were maintained in standard curing room for 28 days before testing, then the specimens were wrapped with HFRP, including CFRP, BFRP and GFRP. The related material properties of the three FRPs were measured by testing and shown in Table 1.

Table 1 Mechanical properties of FRPs

Type of FRP	Tensile strength (MPa)	Elastic modulus (GPa)	Elongation (%)	Thickness (mm)
CFRP	4833	254.16	1.71	0.167
BFRP	1575	83.98	2	0.153
GFRP	1079	69.45	2.23	0.111

2.2 Wrapping and testing method

Following wet lay-up procedure, FRP was wrapped on the surface of columns. All the FRP sheet used for confining the concrete has a width of 300 mm. The overlapping length was set as 150 mm in hoop direction and the overlapping zones were deliberately offset from layer to layer. Two layers of CFRP with 50 mm width were wrapped on the two ends of the HFRP confined column in order to prevent local compressive failure near the ends of columns. Details of specimen are shown in Table 2.

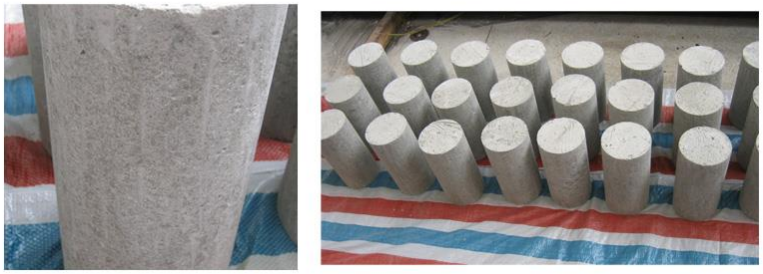

(a) Specimen un-wrapped

(b) Specimen wrapped

Fig. 1 Specimen columns

Table 2 Details of specimens

Specimen	Fiber wrapping approach	Numbers of specimen	Types of FRP
P0	None	3	—
C2	Two layers of CFRP	3	1
B2	Two layers of BFRP	3	1
G2	Two layers of GFRP	3	1
C1B1	One layer of CFRP/One layer of BFRP	3	2
C1B2	One layer of CFRP/Two layers of BFRP	3	2
C1G1	One layer of CFRP/One layer of GFRP	3	2
C1G2	One layer of CFRP/Two layers of GFRP	3	2
B1G1	One layer of BFRP/One layer of GFRP	3	2
C1B1G1	One layer of CFRP/One layer of BFRP/One layer of GFRP	3	3

Note of Table 2: P0 refers to the normal concrete specimen, while B, G and C refer to BFRP, GFRP and CFRP respectively. C1B1 means that the specimen is wrapped by one layer of CFRP and one layer of BFRP from inner to outside, and the others are the same.

Four strain gauges were bonded uniformly on the specimens in longitudinal and hoop directions to record the strains in the two directions respectively. In addition, axial strains were also measured by two linear variable displacement transducers (LVDTs) at 180° apart and covering the mid-height region of 120 mm for both unconfined and confined specimen, as is shown in Fig. 2. The loading was applied by MATEST material testing machine made in Italy, with a displacement control of 0.18 mm per minute.

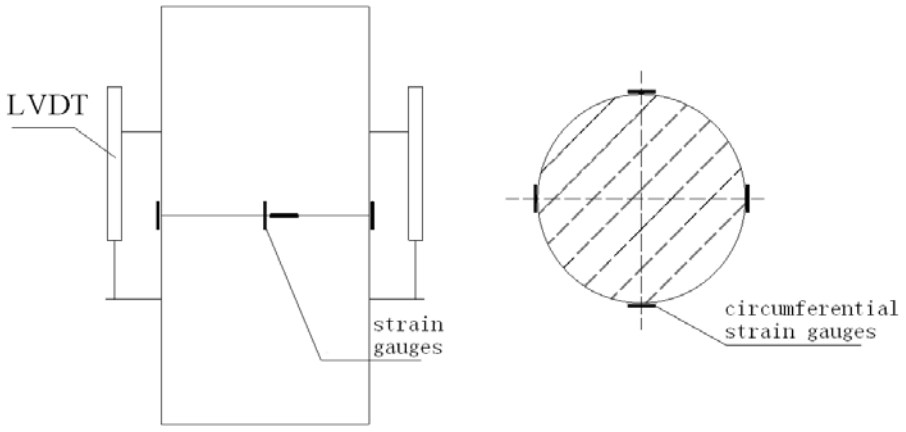

(a) LVDTs and axial strain gauge layout (b) Hoop strain gauge layout
Fig. 2 Arrangement of displacement and strain gauges

3. TEST RESULTS AND ANALYSIS

The load-bearing capacity, hoop and axial strains of concrete columns measured in the test and were shown in Table 3

Table 3 Experimental results

Specimen	Load-bearing capacity (MPa)	Relative value	Longitudinal strain	Relative value	Hoop strain	Relative value
P0	31.72	1.00	3017	1.00	2118	1.00
C2	92.87	2.93	27937	9.26	11173	3.70
G2	47.63	1.50	10805	3.58	12252	4.06
B2	57.29	1.81	13403	4.44	12254	4.06
C1G1	74.19	2.34	20277	6.72	13870	4.60
C1G2	83.81	2.64	21569	7.15	14088	4.67
C1B1	74.73	2.36	20597	6.83	12551	4.16
C1B2	87.77	2.77	24000	7.95	13106	4.34
B1G1	53.12	1.67	12153	4.03	11990	3.97
C1B1G1	75.56	2.38	20153	6.68	12869	4.27

3.1 The failure modes

Sounds arising from FRP rupture could be heard from time to time when the confined concrete columns were loaded to about 80% of its ultimate load-bearing capacity. It can be observed that the rupture of FRP increased with the increase of loads, till the ultimate compressive failure of the confined specimens.

When the failure of columns confined by CFRP occurred, the FRP sheet was quickly fractured into strips, which was accompanied with a loud popping sound and a sharp decrease of the load-bearing capacity, suggesting a typical brittle fracture. Compared with the concrete columns confined by CFRP, cracking sound heard during the failure of the columns confined by BFRP is smaller, which was accompanied by a quick drop of the load-bearing capacity. During the failure process of the concrete columns confined by GFRP, there was no apparent sound arising from FRP rupture (due to the large deformation behavior of GFRP). Instead, the central part of the specimen bulged, leading to the appearance of a number of parallel small cracks on the GFRP sheet; the cracked GFRP region was eventually extended towards to the two ends of columns till rupture of GFRP appeared. The above failure process was quite progressive. So, it can be said that the failure of GFRP confined columns is much more ductile than those confined by CFRP and BFRP. .

For the concrete columns confined by one type of FRP (CFRP/BFRP/GFRP), the fracture of FRP usually happed at the same place on the column. On the other hand, for the concrete columns confined by HFRP, the fibers were tore apart to some extend when fractured, indicating an obvious ductility failure. The failure modes of specimens were shown in Fig. 3.

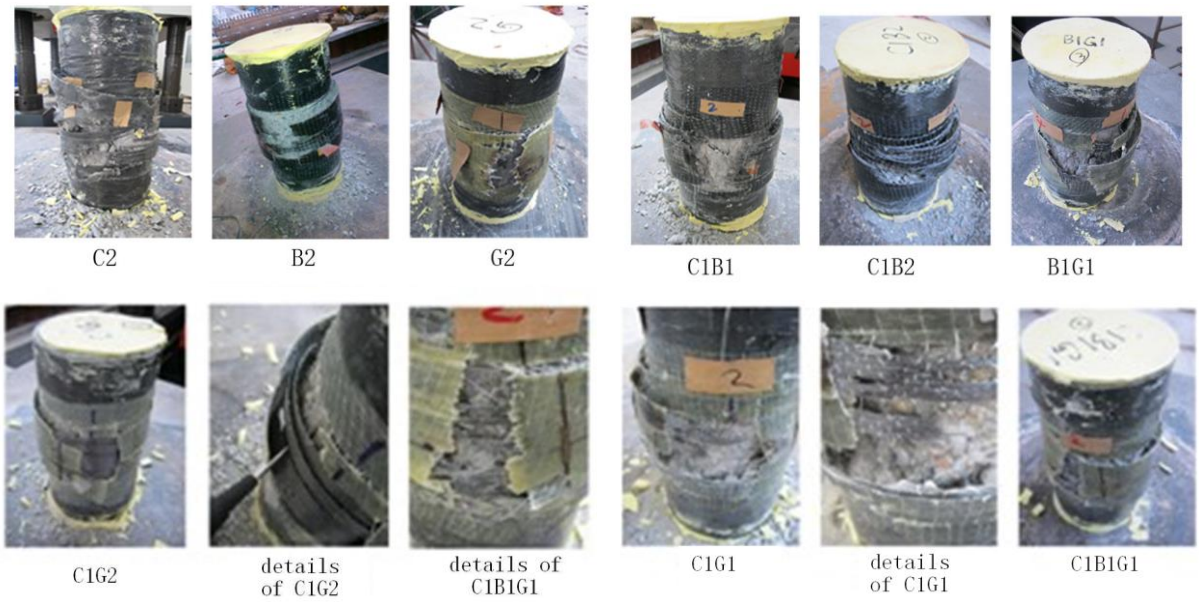

Fig. 3 The failure modes of specimens

For the circular concrete columns confined by HFRP, the inner fiber is ruptured firstly because of lower elongation. The fibers of higher elongation help to prevent cracks in concrete from propagation and carry the additional loads caused by the fracture of the fibers of lower elongation. As a result, a kind of parallel cracks formed within the FRP sheet with higher elongation. Meanwhile, the stress released from the damaged inner layer fibers was transformed to the outer one via the concrete members, which increases the stress of outer fiber. At last, the outer fibers fractured at their weakest section. The different elongations of fibers within the HFRP prevent the sudden rupture of the HFRP as a whole, leading to a progressive rupture process of the HFRP. As a result, the failure of the columns confined with HFRP is generally more ductile than those confined by a single type of FRP.

3.2 Analysis of compressive strength, fiber performance and ductility

Compared with control specimen P0 (without FRP confinement), the compressive strengths of specimens with two layers of fibers, namely C1G1, C1B1and B1G1 are increased by 134%, 136% and 67% respectively (see Table 3). The compressive strength of C1G1 and C1B1 are nearly the same, but the hoop strain of FRP in C1G1 is obviously bigger than that in C1B1, which suggests that if the combination of fiber elongations is appropriate, the confined specimen can take the advantage of the fiber with high elongation and decrease the brittleness of specimens failure caused by rupture failure of FRP, which makes full use of the elongations of different fibers and increases the deformation capacity of specimens.

The strengths of concrete columns confined by three-layer of FRP are higher than that by two-layer. Moreover, the compressive strength of C1G2 and C1B2 is higher than that of C1B1G1; the latter is higher than that of C1B1 only by 1.57 MPa. This

again suggested that the combining application of FRPs has a significant effect on the strength of specimens, but the confining effectiveness will not be significantly increased with the increase of fiber types. It also suggested that three kinds of fibers (or more) may be not suitable to be used together in practice.

The hoop strains of C2, G2 and B2 are 1.11%, 1.23% and 1.22% respectively when FRP rupture happened, while the hoop strains of C1G1 and C1B1 are 1.39% and 1.26%, obviously higher than those of single type fiber (such as C2, G2 and B2), also suggesting that hybrid use of FRPs can make a full use of the high elongation property of some FRP (e.g. GFRP) to enhance the ductility of specimens. However, the hoop strain of B1G1 is lower than those of B2 and G2. A possible explanation is that the elongation gap for the two types of FRPs (BFRP and GFRP) is too small to create the hybrid effect mentioned above; on the contrary, some detrimental effects are triggered and the reasons behind need further research. The hoop strains of the concrete columns confined by three-layer of HFRP, such as C1G2 and C1B2 are higher than that by two-layers, such as C1G1 and C1B1 indicating that with the increase of layers of FRP with higher elongation, the hybrid effect can be fully developed and the ductility of concrete columns confined by HFRP can be improved.

3.3 Effects of FRP layers on stress-strain curves

Stress-strain curves of all specimens are shown in Fig. 4 and Fig. 5. The axial strain is calculated from the readings of LVDT (the average of reading from the two LVDTs), while the hoop strain is calculated by the average value of axial strains from the strain gauges.

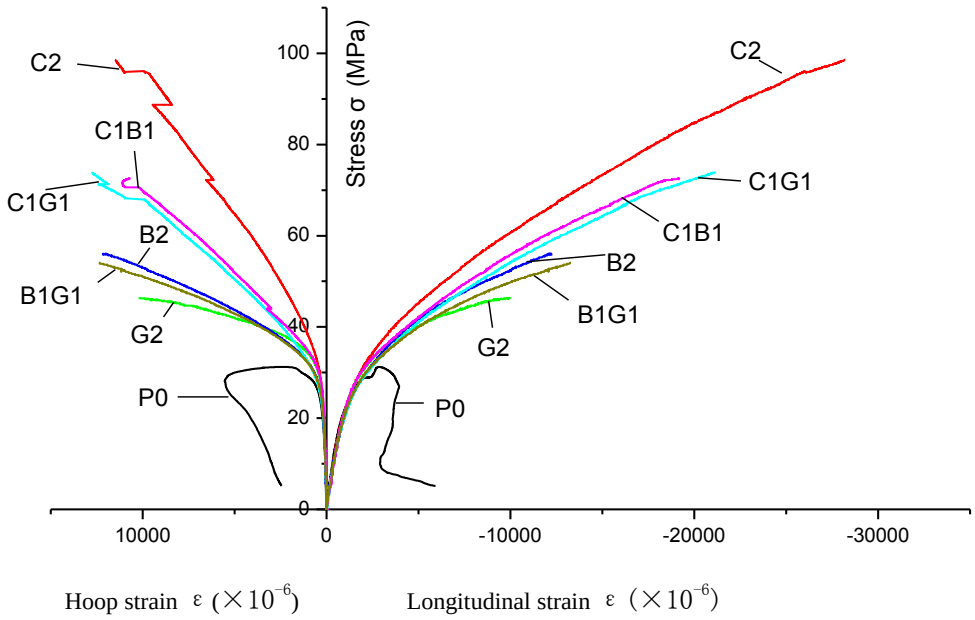

Fig. 4 Stress-strain curves of specimens with 2 layers of FRP

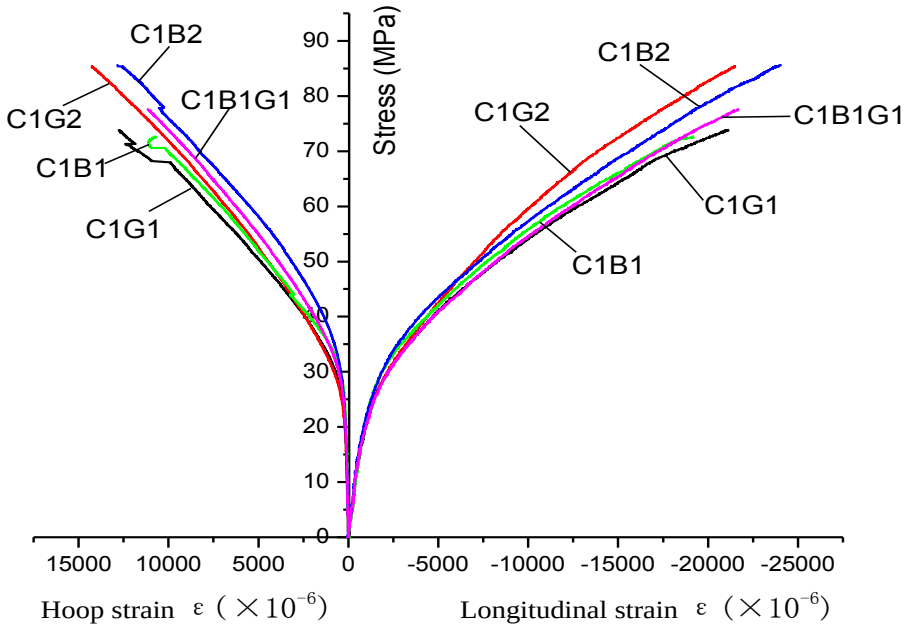

Fig 5 Stress-strain curves of specimens with 3 layers of FRP

It can be seen from Fig. 4 that, compared with columns without FRP (i.e. specimen P0), the stress-strain curves of circular concrete columns confined by FRP are nearly the same when the hoop strain is smaller than peak strain of P0 (strain corresponding the peak strain). The hoop strain of concrete is small before reaching peak strength and will increase greatly after the peak point. This is mainly because, before peak point, the hoop expansion of concrete was very slight (only resulting from Poisson's effect), and thus the confining effect of FRP could not be acted. For the FRP confined concrete column, when the stress can be increased considerably above the peak strength of P0, but the slopes of stress-strain curves (both hoop strains and axial strains) decrease sharply, which are much lower than those of the first segment. As reported (Teng et al. 2002), the curves of the second segment are nearly linear; the slopes of the curves in the second segment are affected by the stiffness of HFRP; and the stress magnitude for the intersection point of the extension line of the second segment of curves with the stress axis is close to the peak strength of P0.

For the concrete columns confined by 2 layers of FRP, the slopes of axial strain are nearly the same. That is to say, the trends of axial strain are similar, but the slopes of hoop strain are significantly different, with trends being affected by the types of hybrid fibers. The stiffness of the axial strain in the reinforced segment can be divided into four groups: (1) C2, (2) C1B1 and C1G1, (3) B2 and B1G1, (4) G2. The slops of the hardening segment of the stress-strain curves decrease from the first group to the fourth group, but the difference is very slight. As to the stress-axial strain curves of columns confined by HFRP, the stiffness in the hardening segment is determined mainly by the fiber of low elongation, but affected by fiber of the high elongation, which

is mainly due to the fact that among the FRPs used in this study, FRP with lower elongation has higher confinement stiffness (in proportional to E_f t_f).

It can be seen from Fig. 5(b) that when columns are confined by 3 layers of FRP (C1G2 and C1B2), the stiffness of the hardening segment is apparently increased as compared with those confined by 2 layers of FRP (C1B1and C1G1), showing that .the effect of confinement can be improved by increasing confining FRP layer. However, compared with that of C1B1, the slope in the hardened segment of C1B1G1 is nearly not increased, which indicates that the increase of the types of FRPs may not have a significant contribution on the confinement. To clarify the reasons for the above complex needs further research.

As for stress-hoop strain curves of columns confined by HFRP, the stiffnesses in the hardening segment are various. It can be seen from Fig. 5 that the hoop stiffness can be sorted as C1B2>C1B1G1>C1G2>C1B1>C1G1 when confinement increased from 2-layer to 3-layer, which matched the order of the confinement stiffness of FRP well.

From the above discussions, it can be concluded that the load-bearing capacity of circular concrete columns confined by HFRP is mainly controlled by the FRPs of low elongation, while the FRPs with high elongation helps to enhance the ductility of columns, thus reduces the speed of development of the hoop strain in the hardening segment and postpones the failure of the specimen.

3.4 Effects of stiffness on stress-strain curves

The performance of specimens in the reinforced segment is affected by the stiffness of hoop strain. The confinement stiffness is defined as

$$K = \frac{\Delta F}{\Delta L} \tag{1}$$

where K is the stiffness, and ΔF and ΔL is the increment of force and displacement respectively. Equation (1) can be rewritten as

$$K = \frac{\Delta F}{\Delta L} = \frac{\frac{\Delta F}{A} A}{\frac{\Delta L}{L} L} = E \frac{th}{L} \tag{2}$$

where, A is the cross-sectional area of HFRP, L is the circumference of HFRP, which is regarded as the same as that of the circumference of specimen approximately, t is the thickness of HFRP, h is height of constraint fibers, which is the same as that of the column, E is the elastic modulus of HFRP.

The confinement stiffness of each group of HFRP can be calculated by Eq. (2), and shown in Table 4.

Table 4 Confinement stiffness of HFRP

Specimen	C2	B2	G2	C1B1	C1B2	C1G1	C1G2	B1G1
Calculation stiffness $\times 10^{12}$ (N/m)	54.18	16.40	9.79	35.29	43.49	31.94	36.95	13.09

It can be seen from Table 4 that the differences in confinement stiffness of group B1G1 and B2, group C1G1 and C1B1, group C1B1G1 and C1B2 are 3.31, 3.35 and 3.33 respectively. The differences of constraint stiffness are very small. The stress-strain curves of the three groups of specimens are shown in Figs. 6-8. The maximum difference of confinement stiffness is 44.39 and is that between C2 and G2. The stress-strain curves of this group of specimens are shown in Fig. 9.

The circular concrete columns have hoop expansion under compression, and their expansion is restricted by FRP. So under the same hoop constraint, the longitudinal strain and stress of concrete columns are the same, and the only difference lies in the rupture strengths of fibers, which are directly related with the ultimate compressive strength of circular concrete columns.

It can be seen from Figs. 6 and 7 that the slopes of stress-strain curves in the hardening segment are almost the same if the difference in confinement stiffness of HFRP is small. However, the compressive strength of confined concrete is different. It can be seen from Fig. 9 that the slopes of the curves in the second segment are obviously different if the confinement stiffness of HFRP varies greatly, which indicates that the slopes of the curves in second segment, namely the hardening segment, are mainly affected by confinement stiffness of HFRP. For example, the difference of the confinement stiffness between C1B1 and C1G2 is only 1.66, so the slopes of their hardening segments are nearly the same, as shown in Fig. 10. The small difference of slop in the later stage can be attributed the higher elongation of the GFRP, which was proved by comparing the hoop fracture strain of the two specimens. So, it can be said that the stress-strain relation curves in the second segment are affected by the elongation capacity of the outer FRP layer which has a significant bearing on the hoop constraint in FRP.

4. STRESS-STAIN MODEL

4.1 Determination of HFRP parameters

The existing studies (Hai and Mutsuyoshi 2012, Rousakis 2012, Mosallam 2012) suggest that the elastic modulus of HFRP is agree well with the theory of mixture, and the equation is as follows

$$E = E_1 V_1 + E_2 V_2 + E_3 V_3 \tag{3}$$

where *E* is the elastic modulus, *V* is the volume fraction of fibers with its subscript representing the fiber type.

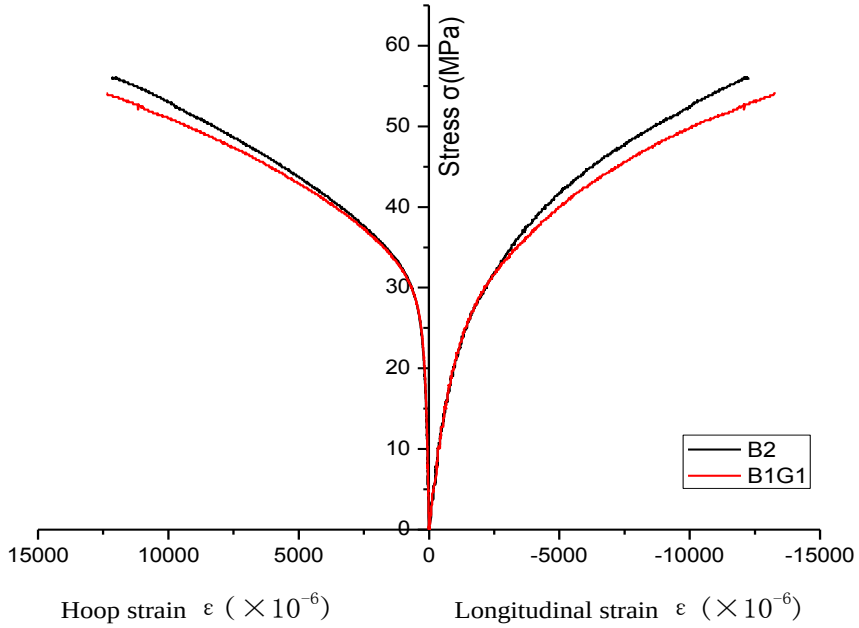

Fig. 6 Stress-strain curves of B2 & B1G1

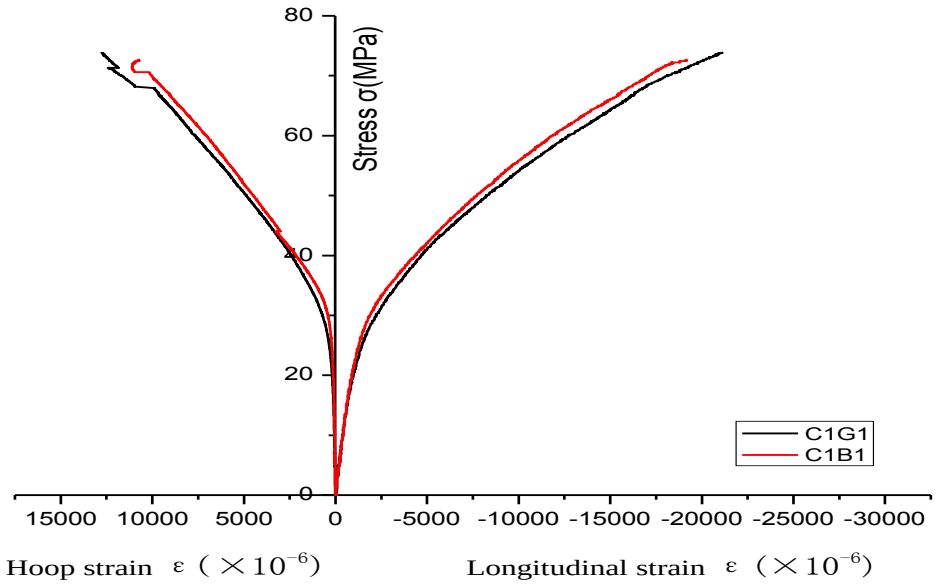

Fig.7 Stress-strain curves of C1G1 & C1B1

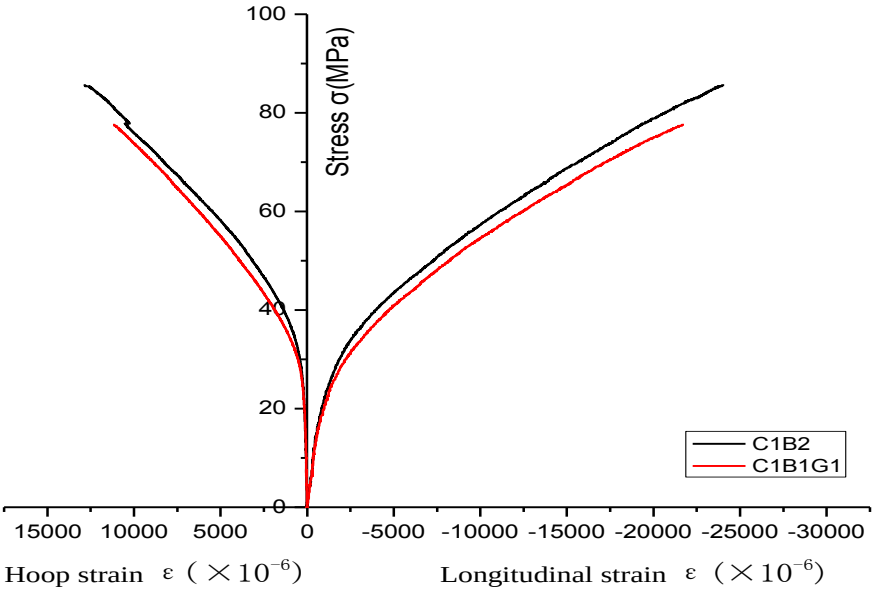

Fig.8 Stress-strain curves of C1B1G1 & C1B2

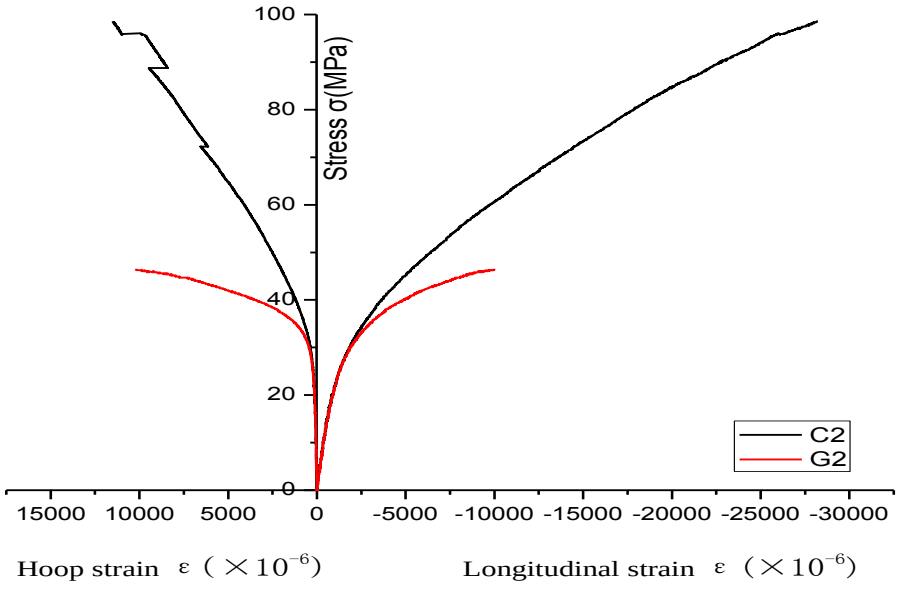

Fig. 9 Stress-strain curves of C2 & G2

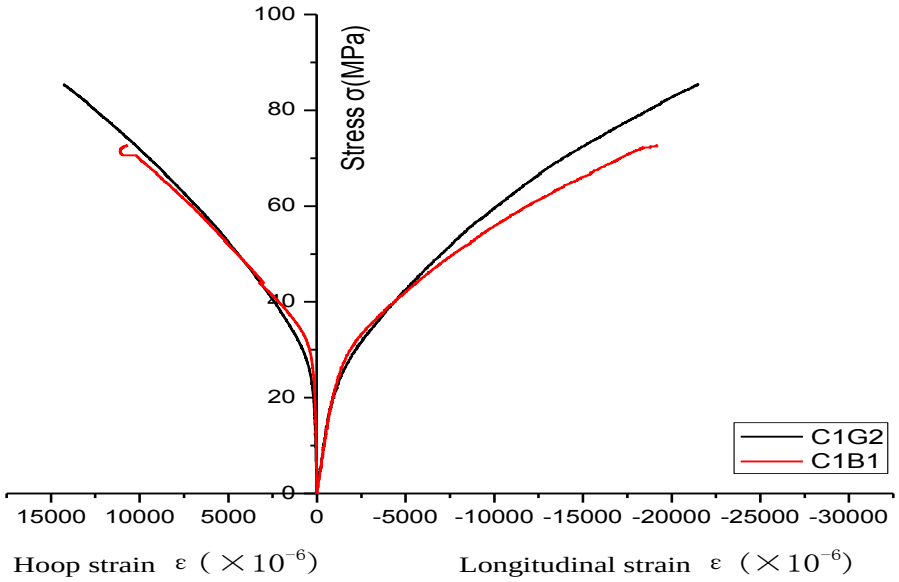

Fig. 10 the Stress-strain curves of C1B1 & C1G2

The elastic modulus of HFRP can be calculated by Eq. (3), and the comparison between the calculated and measured values are shown in Table 5. It can be seen that Eq. (3) provides rather good predictions on the experimental values of elastic modulus for HFRP.

Table 5 Elastic modulus of HFRP

Specimen	C1B1	C1B2	C1G1	C1G2	B1G1	C1B1G1
Measured elastic modulus（GPa）	172.85	143.41	193.68	165.91	96.27	159.41
Calculated elastic modulus（GPa）	172.79	144.06	180.4	149.13	77.87	146.18

The hoop tensile strength of HFRP f_{frp} cannot be calculated by the theory of mixture, but it can be calculated exactly by the coefficient of hybrid effect (Xu 2012), as follows.

$$f_{frp} = E\varepsilon_{le}(1+\mathrm{R_e})S \tag{4}$$

where, E is the elastic modulus of HFRP. ε_{le} is the ultimate elongation of the FRPs with lower elongation. S is the correction factor to account for the difference between

the hoop tensile strength and tensile strength, taken as 0.6; R_e is a hybrid factor and calculated by following formulation:

$$\mathrm{R_e} = T^2 \varphi (1 - V_{le}) \tag{5}$$

where T is the wrapping approach of layers, and is taken as 1 when hybrid among layers were used. φ is the dispersion coefficient V_{le} is the volume fraction of the fibers of lower elongation.

The horizontal expansion takes place in the concrete when concrete columns confined by FRP are under axial compression. The expansion is constrained by FRP, whose confinement effect is affected by the quantity and intensity of FRP as well as the diameter of confined columns, expressed as follows:

$$f_l = \frac{2 f_{frp} t_{frp}}{d} \tag{6}$$

where, t_{frp} is the calculated thickness of FRP, d is the diameter of confined circular concrete columns.

The elastic modulus, lateral constraint and failure strength of HFRP can be calculated from Eq. (3)-(6), and shown in Table 6.

Table 6 Elastic modulus, lateral constraint and failure strength of HFRP

Specimen	E (GPa)	φ	V_{le}	$\mathrm{R_e}$	f_{frp} (MPa)	f_l (MPa)
C2	254.16	—	—	—	4833.50	21.53
B2	83.98	—	—	—	1575.90	6.43
G2	69.45	—	—	—	1175.60	3.48
C1B1	172.79	0.50	0.522	0.2390	2196.53	9.37
C1B2	144.06	0.33	0.353	0.2135	1793.64	11.31
C1G1	180.40	0.50	0.600	0.2000	2221.08	8.23
C1G2	149.13	0.33	0.430	0.1881	1817.88	9.43
B1G1	77.87	0.50	0.580	0.2100	966.72	3.40
C1B1G1	146.18	0.33	0.353	0.2135	1820.03	10.46

4.2 Strength model of concrete confined by HFRP

The following strength model of confined concrete was presented by Richart (Richart et al. 1928) and was directly used to FRP confined concrete by Farids (Farids and Khalili 1982). It is a mostly adopted strength model of concrete confined by FRP at present and is expressed as follows:

$$\frac{f'_{cc}}{f'_{co}} = 1 + k_1 \frac{f_l}{f'_{co}} \tag{7}$$

where, f'_{cc} and f'_{co} refers to the compressive strength of concrete confined and unconfined by FRP separately. f_l is the lateral restraint stress. k_1 is the constraint validity coefficient.

This paper takes a linear regression analysis on the experimental data, and the strength model of concrete confined by FRP is obtained as follows:

$$\frac{f'_{cc}}{f'_{co}} = 1 + 4.88 \frac{f_l}{f'_{co}} \tag{8}$$

Table 7 lists the comparisons between typical strength models and the experimental strengths obtained in the present study, with the statistical indexes of typical strength models listed in Table 8. It can be obtained from Tables 7 and 8 that the strength predicted by the typical strength models is smaller than the tested ones for circular concrete columns confined by HFRP. However, the predicted strength based on Eq. (8) agrees well with the experimental value, with a correlation coefficient of 0.926, an average ratio of 1.016, a standard deviation of 0.068 and a variation coefficient of 0.067.

Table 7 Strength obtained from simulation models and experimental results

Specimen	Test strength (MPa)	This paper model $k_1 = 4.88$	Teng et al. (2002) model $k_1 = 2$	Karbhari and Gao (1997) model $k_1 = 2.1(\frac{f_l}{f'_{co}})^{-0.13}$	Miyauchi et al. (1999) model $k_1 = 2.98$
C1B1	73.99	77.45	50.46	54.78	59.65
C1B2	87.77	86.92	54.34	58.88	65.43
C1G1	74.19	71.9	48.19	52.32	56.25
C1G2	83.81	82.91	52.70	57.16	62.98
B1G1	53.12	50.71	38.53	41.27	41.86
C1B1G1	75.56	82.76	52.64	57.09	62.89

Table 8 Statistical indexes of strength model in this paper

Model	Ratio of test and calculation values		
	Average	Standard deviation	Variation coefficient（%）
Simulation model of this paper	1.016	0.068	6.7
Teng et al. (2002) model	1.517	0.104	6.8
Karbhari and Gao (1997)model	1.144	0.061	5.3
Miyachi et al. (1999) model	1.297	0.071	5.5

4.3 Ultimate axial strain of concrete confined by HFRP

The ultimate axial strain of concrete confined by HFRP is a key parameter of the stress-strain curve. The value of the parameter is related with the lateral restricting stress f_l, as shown in Fig. 11.

Fig. 11 Regression of ultimate axial strain for concrete confined by HFRP

The relationship between dimensionless ultimate axial strain and the constraint ratio is shown in Fig.11. It can be seen that there exists a nearly linear relationship between the ultimate axial strain and constraint ratio. The relationship can be described by the linear regression analysis and is shown by the following Eq. (9):

$$\frac{\varepsilon_{cc}}{\varepsilon_{co}} = 2.61 + 14.4\frac{f_l}{f'_{co}} \tag{9}$$

where, ε_{cc} is the ultimate axial strain of concrete confined by FRP, ε_{co} is the ultimate axial strain of normal concrete.

Fig. 12 Stress-strain relationship of concrete confined by HFRP

4.4 Stress-strain model

To develop a simple but accurate model for the stress-strain relationship for the concrete confined by HFRP, two hypotheses were taken in this paper. Firstly, the intersection point between the extension line of the hardening segment of the stress-strain curve and the stress axis equals to the compressive strength of normal concrete. Secondly, the termination point in the hardening segment expresses both the compressive strength and ultimate axial strain, as shown in Fig. 12.

Based on the above two assumptions, the relationship of axial stress σ_c with axial strain ε can be proposed as follows:

$$\sigma_c = f'_{co}(1-e^{-1000\varepsilon}) + E_2\varepsilon, \text{ when } 0 \le \varepsilon \le \varepsilon_{cc} \tag{10}$$

where, E_2 is the slope of the curve in second segment.

Based on the first assumption, the following formula can be obtained from Fig. 12:

$$E_2 = \frac{f'_{cc} - f'_{co}}{\varepsilon_{cc}} \tag{11}$$

Comparisons between the stress-strain relations predicted by the proposed model and the test results are presented in Fig. 13. It can be seen from Fig. 13 that the

predicted curves agree well with experimental stress-strain curves of concrete confined by HFRP.

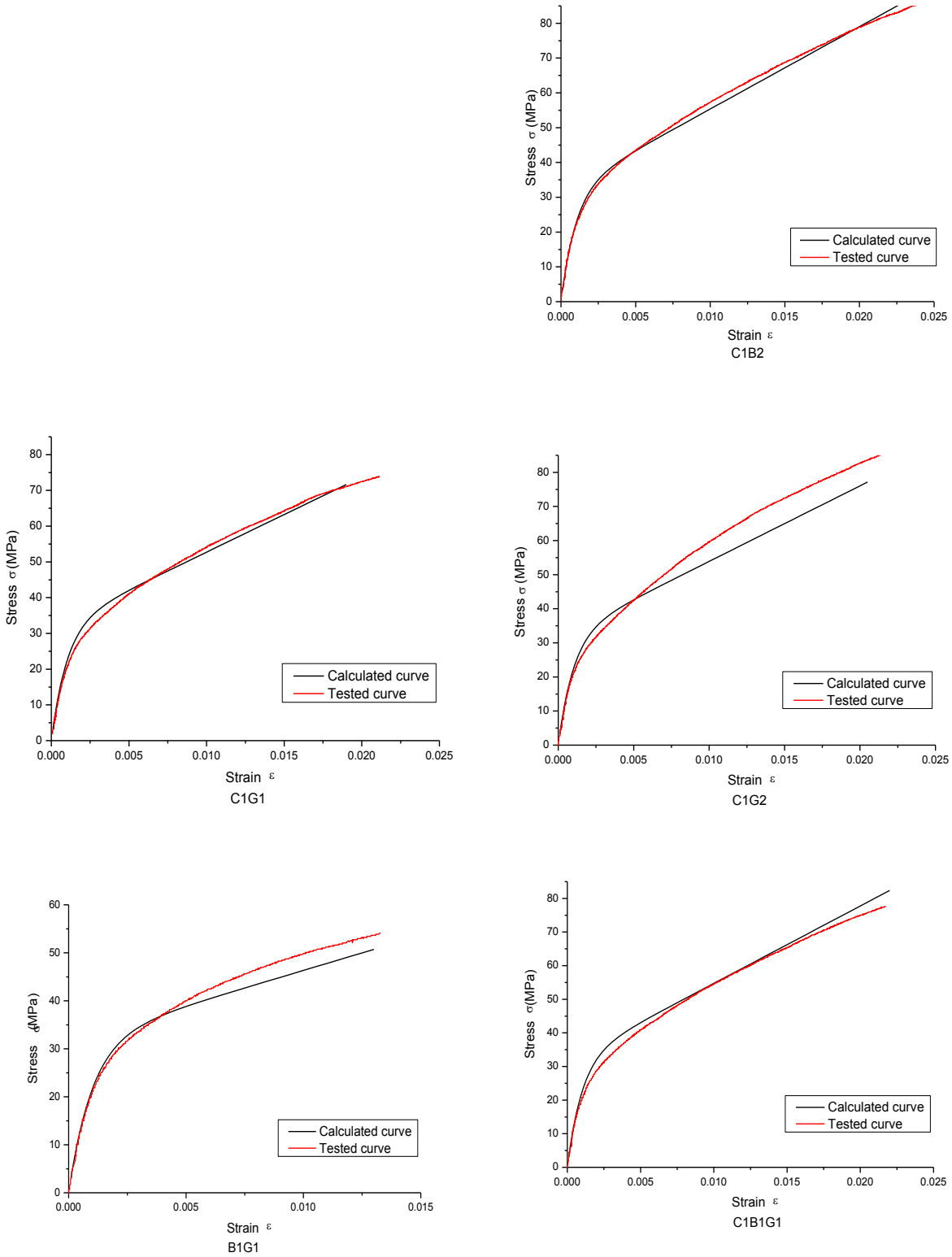

Fig. 13 Stress-strain curves of HFRP confined concrete columns

5. CONCLUSION

This paper first presented an experimental study on the concrete column confined by HFRP. Based on the test results, a modified model was developed to quantitatively describe the stress-strain relationship of the concrete confined by HFRP. From the test results, discussions and comparisons presented in the present study, the follow conclusions can be drawn:

(1) Hybrid use of FRPs can improve the ductility of the concrete confined by FRP subjected to compression load. The rupture strain of hybrid FRP confined concrete columns can be obviously improved than that of single fiber confined columns. The failure of columns can be delayed by reducing the speed of the development of hoop strain. On the other hand, the stiffness of circular concrete columns confined by HFRP can be improved by taking the advantage of the large stiffness of carbon fibers.

(2) The stress-strain model of concrete confined by HFRP presented in this paper matches the experimental results well. It is clearly aware that the model has been substantiated only against very limited test data, so much more test data are required for the improvement/validation of the proposed model.

(3) When three kinds of FRPs were used to confine concrete, the hybrid effect is reduced, suggesting that there should be a limitation on the number of types of FRPs used in the HFRP.

ACKNOWLEDGMENTS

This research was funded by the National Natural Science Foundation of China (Project No. 51278129) and the Foundation of Guangdong Provincial Transportation Department (Project No. 2012-04-013). The foundations are greatly appreciated.

REFERENCE

Bouchelaghem, H., Bezazi, A., Scarpa, F. (2011), “Compressive behaviour of concrete cylindrical FRP-confined columns subjected to a new sequential loading technique”, *Compos. Part B-Eng.* **42**(7), 1987-1993

Chen G.M., Chen, J.F., Teng, J.G. (2012), “Behaviour of FRP-to-concrete interfaces between two adjacent cracks: A numerical investigation on the effect of bondline damage”, *Constr. Build. Mater.*, **28**, 584-591

Chen, W.F. (1982), *Plasticity in reinforced concrete,* McGraw-Hill.

Chen, Z.F., Wan. L.L., Lee. S. (2008), “Evaluation of CFRP, GFRP and BFRP material systems for the strengthening of RC slabs”, *J. Reinf. Plast. Compos.*, **27**(12), 1233-1243

Farids, M.N. and Khalili, H. (1982), “FRP-Encased concrete as a structural material”, *Magaz. Concr. Res.* **34**(121), 191~202.

Guo, Y.C. Huang, P.Y., Yang, Y. and Li, L.J. (2009), “Experimental studies on axially loaded concrete columns confined by different materials”, *Key Eng. Mater.*, 400-402, 513-518

Guo, Y.C., Li, L.J., Chen, G.M., Huang, P.Y. (2012), “Influence of hollow imperfections in adhesive on the interfacial bond behaviors of FRP-plated RC beams”, *Constr. Build. Mater.*, **30**, 597-606

Hosny, A., Shaheen, H., Abdelrahman, A., Elafandy, T. (2006), “Performance of reinforced concrete beams strengthened by hybrid FRP laminates”, *Cem. Concr. Compos.*, **28**(10), 906–913

Hu, H.T., Schnobrich, W.C. (1989), “Constitutive modelling of concrete by using nonassociated plasticity”, *J. Mater Civil Eng ASCE*, **1**(4):199-216.

Hu, H.T., Schnobrich, W.C. (1990), “Nonlinear analysis of cracked reinforced concrete”. *ACI Struct. J.*, **87**(2), 199-207.

Karbhai, V.M and Gao, Y. (1997), “Composite jacketed concrete under uniaxial compression-verifi cation of simple design equations”, *J. Mater. Civil Eng. ASCE*, **9**(4), 185-193.

Lau, D., Pam, H.J. (2010), “Experimental study of hybrid FRP reinforced concrete beams”, *Eng. Struct.*, **32**, 3857-3865

Li, J., Samali, B., Ye, L., Bakoss, S. (2002), “Behaviour of concrete beam–column connections reinforced with hybrid FRP sheet”, *Compos. Struct.*, **57** (1-4), 357-365.

Li, L.J., Guo, Y.C., Huang, P.Y., Liu, F., Deng. J., Zhu, J. (2009), “Interfacial stress analysis of RC beams strengthened with hybrid CFS and GFS”, *Constr. Build. Mater.*, **23**(6), 2394-2401.

Meier, U., Deuring, M., Meier, H., Schwegler, G, (1993), *Strengthening of structures with advanced composites. Alternative materials for reinforcement and prestressing of concrete*, Glasgow, Scotland: J.L. Clarke/Chapman & Hall.

Meyer, C., Okamura, H. (1986), “Finite element analysis of reinforced concrete structures”, ASCE. New York

Miyauchi, K., Inoue, S. and Kuroda, T. and Kobayashi, A. (1999), “Strengthening effects of concrete columns with carbon fiber sheet”, *J. Trans. Jpn. Concr. Inst*., **21**, 143-150.

Mosallam, A., Taha, M.M.R., Kim, J.J., Nasr, A. (2012), “Strength and ductility of RC slabs strengthened with hybrid high-performance composite retrofit system”, *Eng. Struct.*, **36**, 70-80

Richart F.E., Brandtzaeg A., Brown R.L. (1928), “A study of the failure of concrete under combined compressive stresses”. University of Illinois. Engineering Experiment Station. Bulletin; no. 185

Rousakis, T.C., Karabinis, A.I. (2012), “Adequately FRP confined reinforced concrete columns under axial compressive monotonic or cyclic loading”, *Mater. Struct.*, **45**(7), 957-975

Saadatmanesh H., Ehsani M.R. (1991), “RC beams strengthened with FRP plates II: analysis and parametric study”, *J. Struct Eng ASCE*, **117**(11):3434–55.

Samaan, M., Mirmira, A., Shahawy, M. (1998), “Model of concrete confined by fiber composites”, *J. Struct. Eng. ASCE*, **126**(9), 1025~1031.

Sundarraja, M,C., Prabhu, G.G. (2012), “Experimental study on CFST (concrete filled steel tubular) members strengthened by CFRP composites under compression”, *J. Constr. Steel Res.*, **72**, 75-83

Teng, J.G., Chen, .J.F., Smith, S.T., Lam, L. (2002), *FRP-Strengthened RC Structures*, John Wiley & Sons, Ltd.

Teng, J.G., Zhao, J.L., Yu, T., Li, L.J. and Guo, Y.C. (2012), “Recycling of coarsely-crushed concrete for use in FRP tubular columns”. *Proceedings of the First International Conference on Performance-based and Life-cycle Structural Engineering,* December, HongKong. 1389-1397

Vanaja, A., Rao, RMVGK. (2002), “Fibre fraction effects on thermal degradation behaviour of GFRP, CFRP and hybrid composites”, *J. Reinf. Plast. Compos.*, 21(15), 1389-1398

Vecchio, F.J., Collins, M.P. (1986), “The modified compression-field theory for reinforced concrete elements subjected to shear”, *ACI Struct. J.*, 83, 219-231.

Xu S.D. (2012), “*Study on mechanical properties of concrete circular column confined by HFRP under axial compression*”, Dissertation of Master of Science Guangdong University of Technology.

Zhao, J.L., Teng, J.G., Yu T., and Li, L.J. (2013), “Experimental behavior of FRP-concrete-steel double-skin tubular beams”, *11th International Symposium on Fiber Reinforced Polymers for Reinforced Concrete structures*, June, Guimarães, Portugal